CHALMERS
FINITE ELEMENT CENTER

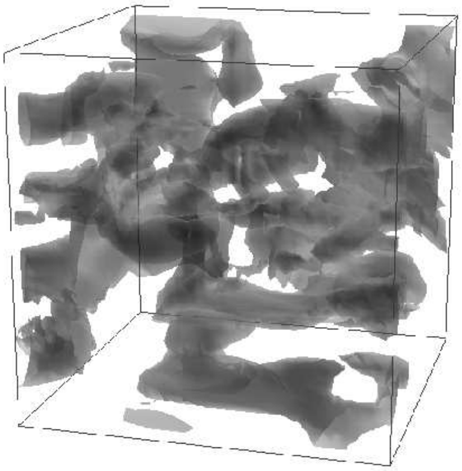

PREPRINT 2002–04

A Computational Study of Transition to Turbulence in Shear Flow

Johan Hoffman and Claes Johnson

Chalmers Finite Element Center
CHALMERS UNIVERSITY OF TECHNOLOGY
Göteborg Sweden 2002

CHALMERS FINITE ELEMENT CENTER

Preprint 2002–04

A Computational Study of Transition to Turbulence in Shear Flow

Johan Hoffman and Claes Johnson

CHALMERS

Chalmers Finite Element Center
Chalmers University of Technology
SE–412 96 Göteborg Sweden
Göteborg, February 2002

A Computational Study of Transition to Turbulence in Shear Flow
Johan Hoffman and Claes Johnson
NO 2002–04
ISSN 1404–4382

Chalmers Finite Element Center
Chalmers University of Technology
SE–412 96 Göteborg
Sweden
Telephone: +46 (0)31 772 1000
Fax: +46 (0)31 772 3595
www.phi.chalmers.se

Printed in Sweden
Chalmers University of Technology
Göteborg, Sweden 2002

A COMPUTATIONAL STUDY OF TRANSITION TO TURBULENCE IN SHEAR FLOW

JOHAN HOFFMAN AND CLAES JOHNSON

Abstract. We present a computational study of transition to turbulence in Couette and Poiseuille flow on the unit cube, with periodic boundary conditions in the streamwise x_1-direction. We identify an initial phase with slow, linear, x_1-independent pertubation growth of the streamwise velocity, followed by rapid growth of x_1-dependent pertubations of both streamwise and transversal velocities. We analyze the linear pertubation growth, and we model the transition scenario in a simple ODE system.

1. Introduction

The phenomenon of transition from laminar to turbulent flow, studied intensively by Reynolds more than hundred years ago in the case of pipe flow, has long been an outstanding open problem in science, where today computational methods shed new light. Reynolds observed by injecting dye into water flowing through a transparent pipe, that sometimes the flow changed quite abruptly from organized laminar to turbulent fluctuating flow at some point downstream from the inlet, with the transition being identified by the deviation of the dye from a straight line into a rapidly fluctuating path. Seemingly similar sudden changes may be observed in the raising smoke from a cigarett, or in a stock market crash, or a sudden break up of a long-lasting marriage.

The basic question in all these cases is: why does the transition take place at a specific point in space or time, or not at all? Observing the straight line of the dye in Reynolds experiment before the transition, does not appear to give any signal of emerging instability, and a stock market crash necessarily must be a surprise for the majority of the market actors. The research on transition to turbulence in fluid flow has largely focussed on finding a relation between the Reynolds number and transition, with ideally a so called critical Reynolds number for each type of flow, identified by the fact that transition to turbulence takes place if and only if the actual Reynolds number is larger than the critical Reynolds number. Reynolds himself had little reason to belive in the existence of such critical Reynolds numbers noting that in his own experiments the transition took place in one pipe and not in another at the same Reynolds number. Nevertheless, most text books in fluid mechanics today present critical Reynolds numbers for various flows, such as 5772 for Pouiseuille flow between two parallel fixed plates (with parabolic velocity profile), and

Date: February 28, 2002.

Department of Mathematics, Chalmers University of Technology, S–412 96 Göteborg, Sweden, *email*: hoffman@math.chalmers.se
email: claes@math.chalmers.se .

∞ for Couette flow between two moving parallel plates (with linear velocity profile), both however at severe variance with experiments. For example, Couette flow may go turbulent in experiments for a wide range of Reynolds numbers starting at around 300, depending on the experimental set-up, and similarly Pouiseuille flow starting around 1000. The stated critical Reynolds numbers come out of a so called normal mode stability analysis of 2d linearized equations, referred to as the Orr-Sommerfeld equations, based on identifying exponentially growing eigenmodes. The striking difference in the theoretical predictions and the practical experiments for transition in parallel flow, has driven the classical study of hydrodynamic stability into a severe crisis.

However, during the last decades new insight on the importance of 3d perturbations and non-modal growth has been developing, see [3], giving a better understanding of the process of transition from laminar to turbulent flow in almost parallel flow, such as pipe flow and boundary layer flow. We will present pieces of this new picture using a quantitative mathematical/computational analysis of hydrodynamic stability. In particular, the analysis will show that even if the dye injected into the pipe indicates that fluid particles follow (almost) straight lines prior to the transition, the flow actually gets considerably reorganized as a necessary preparation before the transition. We will refer to the reorganization as resulting from the *Taylor-Görtler mechanism* through which small transversal velocity perturbations after some time result in big perturbations in the streamwise velocity, which is the initial and crucial phase of the transition process, and which results from the non-normality of the linearized Navier-Stokes equations when linearized at parallel flow. Of course we may expect to find similar reorganizations preparing transitions into stock market and marriage crashes.

A possible reason for the survival of the classical misleading normal mode stability analysis for parallel flow, despite its lack of experimental support, is probably the fact that there are some other cases, where the same type of analysis in fact is correct and conforms with experiments, namely the *bifurcating* Benard and Taylor-Couette flows, changing from one configuration to another at a certain well defined Reynolds number. The bifurcation of Bernard flow involves the development of organized patterns of convective rolls of fluid in motion. A bifurcation involves a change from one configuration loosing stability, to a new stable configuration, which is different from the process of transition to turbulence, with the new configuration being increasingly unstable. Now, a bifurcation in general may be detected through a normal mode analysis based on finding for the linearized equations an eigenvalue with zero real part. In particular, the critical Reynolds number for the first bifurcations in Taylor-Couette and Bernard flow, may be found analytically this way. As indicated this approach does however not work for parallel Couette or Poiseuille flow, which do not bifurcate to find new stable configurations, but instead go into turbulent unstable motion. It appears that the success of the mathematical theory in the bifurcating cases, has overshadowed the failure in the non-bifurcating cases.

2. Hydrodynamic stability

Hydrodynamic stability concerns the quantitative stability properties of the incompressible Navier-Stokes equations, which are of basic importance for the understanding of phenomena of fluid flow such as bifurcation or transition to turbulence. The incompressible Navier-Stokes equations expressing conservation of momentum and incompressibility of a unit density constant temperature Newtonian fluid with constant kinematic viscosity $\nu > 0$ enclosed in a volume Ω in $\mathbb{R}^3$, take the form: find (u, p) such that

$$\begin{aligned} D_{u,t}u - \nu\Delta u + \nabla p &= f && \text{in } \Omega \times I, \\ \operatorname{div} u &= 0 && \text{in } \Omega \times I, \\ u &= w && \text{on } \partial\Omega \times I, \\ u(\cdot, 0) &= u^0 && \text{in } \Omega, \end{aligned} \tag{2.1}$$

where $u(x,t) = (u_i(x,t))$ is the *velocity* vector and $p(x,t)$ the *pressure* of the fluid at (x,t), and f, w, u^0, $I = (0,T)$, is a given driving force, Dirichlet boundary data, initial data and time interval, respectively. Further,

$$D_{u,t}v = \dot{v} + (u \cdot \nabla)v \tag{2.2}$$

is the *particle derivative* of $v(x,t)$ measuring the rate of change $\frac{d}{dt}v(x(t),t)$ of $v(x(t),t)$ along the trajectory $x(t)$ of a fluid particle with velocity u, satisfying $\dot{x}(t) = u(x(t),t)$, where as usual $\dot{v} = \partial v/\partial t$.

We assume that (2.1) is normalized so that the reference velocity and typical length scale are both equal to one. The Reynolds number Re is then equal to ν^{-1}. Of course, the specification of the length scale may not be very obvious and thus the Reynolds number may not have a very precise quantitative meaning.

2.1. The linearized Navier-Stokes equations.

The basic study of hydrodynamic stability concerns the linearized Navier-Stokes equations for perturbations (φ, q) of a given solution (u,p) of (2.1) corresponding to the initial data u_0 and right hand side f, obtained by subtracting (u,p) from the solution $(u+\varphi, p+q)$ corresponding to the perturbed initial data $u^0 + \varphi^0$ and right hand side $f + g$, and omitting the quadratic perturbation term $(\varphi \cdot \nabla)\varphi$:

$$\begin{aligned} D_{u,t}\varphi + (\varphi \cdot \nabla)u - \nu\Delta\varphi + \nabla q &= g && \text{in } \Omega \times I, \\ \nabla \cdot \varphi &= 0 && \text{in } \Omega \times I, \\ \varphi &= 0 && \text{on } \partial\Omega \times I, \\ \varphi(\cdot, 0) &= \varphi^0 && \text{in } \Omega, \end{aligned} \tag{2.3}$$

where $(\varphi \cdot \nabla)u = (\sum_{j=1}^3 \varphi_j u_{i,j})_{i=1}^3$ with $v_{,j} = \partial v/\partial x_j$.

The basic question in hydrodynamic stability is to estimate the solution (φ, q) of (2.3) in various norms in terms of appropriate corresponding norms of the data (g, φ_0), for example in terms of certain *stability factors*. A basic example is given by the *weak stability factor* $S_0(u, T, \varphi^0)$ depending on the base flow u, final time T and the perturbation φ^0, defined by

$$S_0(u,T,\varphi^0) = \frac{\|\varphi\|_I}{\|\varphi^0\|}, \tag{2.4}$$

or the factor $S_0(u,T)$ depending on the base flow u and the final time T with a maximization over all perturbations, defined by

$$S_0(u,T) = \sup_{\varphi^0\in L_2} \frac{\|\varphi\|_I}{\|\varphi^0\|}, \tag{2.5}$$

where φ is the solution of (2.3) with $g = 0$ and initial data $\varphi^0 \neq 0$, and $\|v\| = \|v\|_{L_2(\Omega)}$, $\|v\|_I = \sup_{0<t<T} \|v(\cdot,t)\|$. The factor $S_0(u,T,\varphi^0)$ measures the growth over the time interval $(0,T)$ of the perturbation φ^0 of initial data, and the factor $S_0(u,T)$ measures the maximal growth over the time interval $(0,T)$ of an initial perturbation of initial data. We refer to these stability factors as *weak* because we measure the solution itself and not derivatives thereof.

We now give estimates of the stability factor $S_0(u,T)$ in two extreme cases: a *worst case* with exponential dependence in KT related to non-smooth turbulent flow, where K is a measure of the gradient, and a *best case* with linear dependence in KT related to smooth laminar flow. Assuming that $K = 1$ and $T = \nu^{-1} = Re$, the dependence can be expressed as an exponential or linear dependence in the Reynolds number Re, with the exponential dependence indicating instability even for moderately large Reynolds numbers, while the linear dependence corresponds to a smooth laminar flow.

2.2. **Worst case exponential perturbation growth.** Multiplying the first equation of (2.3) by φ and integrating over $\Omega \times (0,t)$, using the incompressibility of both u and φ, one gets for $t > 0$:

$$\|\varphi(\cdot,t)\|^2 \le -2\int_0^t \int_\Omega (\varphi\cdot\nabla)u\cdot\varphi\, dxds + \|\varphi^0\|^2,$$

from which follows by the Grönwall inequality that $S_0(u,T) \le \exp(CKT)$, with $C \approx 1$, which is a worst case exponential estimate. We note the exponential growth is generated by the presence of the zero order term $(\varphi\cdot\nabla)u$, as in the simple scalar ode $\dot\psi = K\psi$ with solution $\psi(t) = \psi(0)\exp(Kt)$. A flow with this very strong perturbation growth cannot exist as a stable flow. Since there are some more or less stable flows observable in nature, it must be possible in special cases to obtain reduced growth rates by using particular features of the zero order coupling term $(\varphi\cdot\nabla)u$. A basic such case arises in shear flow, with a particular coupling of the perturbations of the velocities in streamwise and transversal directions, which we now turn to.

2.3. **Linear perturbation growth in shear flow.** *Shear flow* is a basic type of flow, occuring in pipe flow and boundary layer flow, where the streamlines are almost parallel straight lines and the transversal variation of the streamline flow velocity is balanced by a shear force. We now show that for such flows the weak stability factor $S_0(u,T)$ defined by (2.5) satisfies $S_0(u,T) \approx KT$. This estimate underlies the first crucial step in the scenario of transition to turbulence in shear flow to be presented, showing that a perturbation growth $\approx \nu^{-1}$ over time intervals of length $T = \nu^{-1}$ is possible even if for smooth flows with $K = 1$, indicating that a small initial perturbation (of size ν say) in fact may cause the base flow to change significantly if we only wait long enough (over a time interval $\approx \nu^{-1}$).

We consider a smooth parallel stationary base flow (u, p) in an infinitely long straight pipe $\Omega = \mathbb{R} \times \omega$, where ω in the (x_2, x_3)-plane is the cross-section (with smooth boundary) of the pipe of diameter of size 1, and the axis of the pipe is oriented along the x_1-axis, and u vanishes on the boundary of the pipe. We assume that the base flow (u, p) is independent of x_1 and satisfies the following assumptions

$$\|u_1\| \approx 1, \qquad \|\bar\nabla u_1\|_\infty = C, \qquad \|\bar u\|_\infty + \|\bar\nabla \bar u\|_\infty \leq c\nu, \tag{2.6}$$

where $\|\cdot\|_\infty$ denotes the maximum norm, $\bar u = (u_2, u_3)$, and $\bar\nabla = (\partial/\partial x_2, \partial/\partial x_3)$ is the gradient with respect to (x_2, x_3). Here and below, c and C denote positive constants of moderate size, which are independent of ν. The assumption (2.6) including a smooth streamwise velocity $u_1 \approx 1$ in the x_1 direction being independent of x_1, and smooth small transversal velocities $\bar u$ of size $\approx \nu$, may be viewed as a basic characteristic of shear flow. A further characteristic may be that the derivatives in the streamwise direction x_1 are one order smaller in ν, so that $u_{1,1} \sim \nu$ and $u_{2,1}, u_{3,1} \sim \nu^2$. We will return to this feature below in the presentation of the scenario of transition to turbulence in Section 3. We further assume as already indicated that $T \sim 1/\nu = Re$.

Assuming that also the perturbation (φ, q) are independent of x_1, the linearized equations (2.3), take the following form:

$$\begin{aligned} D_{u,t}\varphi_1 + (\bar\varphi \cdot \bar\nabla)u_1 - \nu\Delta\varphi_1 &= 0 && \text{in } \omega \times I, \\ D_{u,t}\bar\varphi + (\bar\varphi \cdot \bar\nabla)\bar u + \bar\nabla q - \nu\Delta\bar\varphi &= 0 && \text{in } \omega \times I, \\ \bar\nabla \cdot \bar\varphi \equiv \varphi_{2,2} + \varphi_{3,3} &= 0 && \text{in } \omega \times I, \\ \varphi &= 0 && \text{on } \partial\omega \times I, \\ \varphi(\cdot, 0) &= \varphi_0 && \text{on } \omega. \end{aligned} \tag{2.7}$$

These equations have a very particular structure. First, the equations for the transversal velocity $\bar\varphi$ are fully decoupled from the equation for the streamwise velocity φ_1, and have zero order terms with small coefficients because $|\bar\nabla \bar u| \leq c\nu$. Secondly, the zero order term $(\bar\varphi \cdot \bar\nabla)u_1$ in the equation for φ_1 does not contain φ_1, because $u_{1,1} = 0$. This means that the zero order terms in (2.7) have a special form, which makes it possible to reduce the general worst case exponential growth of $S_0(T)$, to a linear growth. The basic structure of the equations (2.7) is present in the system of ordinary differential equations $\dot\varphi_1 - \varphi_2 = 0$, $\dot\varphi_2 = 0$, for $t > 0$, $\varphi^0 = (0, \varphi_2^0)$ with solution $\varphi_1(t) = t\varphi_2^0$, $\varphi_2(t) = \varphi_2^0$, showing a linear growth of φ_1. The growth in this system is very different from the exponential growth obtained changing the first equation to $\dot\varphi_1 - \varphi_1 = 0$, with the exponentially growing solution $\varphi_1(t) = \exp(t)\varphi_1^0$, assuming now $\varphi_1^0 \neq 0$. Clearly, the change from linear to exponential growth is related to the nature of the coupling, with the direct coupling $\dot\varphi_1 = \varphi_1$ being much stronger than the indirect coupling $\dot\varphi_1 = \varphi_2$, where $\dot\varphi_2 = 0$.

We now prove a basic estimate giving a linear growth bound in time of the streamwise velocity perturbation φ_1 generated by a small transversal perturbation $\bar\varphi^0$. We refer to the physical phenomena causing this perturbation growth as the *Taylor-Görtler mechanism*, which has a crucial role in transition to turbulence. The bound is based on an energy estimate using the decoupling of φ_1 and $\bar{\varphi}$, resulting from the fact that $q_{,1} = 0$ and $\varphi_{1,1} = 0$. Below we present computations showing that the bound is sharp and that linear perturbation growth actually occurs.

Theorem 1. *The stability constant $S_0(u,T)$, defined by (2.5) in the context of x_1-independent pipe flow (u,p) satisfying (2.6), satisfies the following bound for $T = \nu^{-1}$:*

$$S_0(u,T) \leq C\nu^{-1}, \tag{2.8}$$

where C depends on the constant c in (2.6). If the constant c is small enough, then the estimate (2.8) holds for $T \geq \nu^{-1}$ with ν^{-1} replaced by T.

Proof. First, multiplying the equation for $\bar{\varphi}$ by $\bar{\varphi}$, and integrating over ω using the fact that $\bar{\nabla} \cdot \bar{u} = \bar{\nabla} \cdot \bar{\varphi} = 0$, shows that

$$\frac{1}{2}\frac{d}{dt}\|\bar{\varphi}\|^2 + \nu\|\bar{\nabla}\bar{\varphi}\|^2 \leq c\nu\|\bar{\varphi}\|^2.$$

Using Grönwall's inequality, we then find that

$$\|\bar{\varphi}(\cdot,t)\|^2 \leq \exp(C\nu t)\|\bar{\varphi}^0\|^2, \qquad 0 < t \leq T.$$

Next, multiplying the equation for φ_1 by φ_1 and using again the fact that $\bar{\nabla}\cdot\bar{u} = \bar{\nabla}\cdot\bar{\varphi} = 0$, we get

$$\frac{1}{2}\frac{d}{dt}\|\varphi_1\|^2 + \nu\|\bar{\nabla}\varphi_1\|^2 \leq C(\frac{1}{2}\nu\|\varphi_1\|^2 + \frac{1}{2}\nu^{-1}\|\bar{\varphi}\|^2),$$

from which the desired estimate follows by integration. The modification with c sufficiently small is straight forward. □

A challenge is to extend the above result to different base flows (u,p) with slight x_1-dependence. As a small contribution to this problem we present the following example: we assume in addition to (2.6) that

$$\|u_{1,1}\|_\infty \leq c\nu, \qquad \|\bar{u}_{,1}\|_\infty \leq c\nu^2, \tag{2.9}$$

where c is a positive constant, and we allow the perturbation velocity φ to depend on x_1, but we assume for the pressure part q that $q_{,1} = 0$ and that correspondingly the incompressibility condition reduces to $\varphi_{2,2} + \varphi_{3,3} = 0$, which corresponds to a slight compressibility of the original fluid with a pressure perturbation q, which is constant in the x_1-direction. In this case the linearized perturbation equations take the form:

$$\begin{array}{rcll} D_{u,t}\varphi_1 + (\varphi\cdot\nabla)u_1 - \nu\Delta\varphi_1 &=& 0 & \text{in } \Omega\times I,\\ D_{u,t}\bar{\varphi} + (\varphi\cdot\nabla)\bar{u} + \bar{\nabla}q - \nu\Delta\bar{\varphi} &=& 0 & \text{in } \Omega\times I,\\ \varphi_{2,2} + \varphi_{3,3} &=& 0 & \text{in } \Omega\times I,\\ \varphi &=& 0 & \text{on } \partial\Omega\times I,\\ \varphi(\cdot,0) &=& \varphi_0 & \text{on } \Omega, \end{array}$$

which again decouples and thus is amenable to analysis as above.

Remark 2. *The Orr-Sommerfeld equations are the linearized Navier-Stokes equations linearized at x_1-directed parallel flow $u = (u_1(x_2), 0, 0)$ between two parallel plates with normal in the x_2 direction, assuming the perturbations are independent of the transversal direction x_3 parallel to the plates and also that $\varphi_3 = 0$: find $(\varphi(x_1, x_2, t), p(x_1, x_2, t)$ such that for $|x_2| < d$, $x_1 \in \mathbb{R}$, $t > 0$*

$$\begin{aligned} \dot{\varphi}_1 + u_{1,2}\varphi_2 - \nu\Delta\varphi_1 + p_{,1} &= 0, \\ \dot{\varphi}_2 - \nu\Delta\varphi_2 + p_{,2} &= 0, \\ \varphi_{1,1} + \varphi_{2,2} &= 0, \end{aligned} \tag{2.10}$$

with $\varphi(x_1, \pm d) = 0$, and the initial condition $\varphi(x_1, x_2, 0) = \varphi^0(x_1, x_2)$, and where $2d$ is the distance between the plates. In the case of Couette flow $u_1(x_2) \propto x_2$ and for Pouiseuille flow $u_1(x_2) \propto (1 - (x_2/d)^2)$. The stability factor $S_0(u, T)$ turns out to be much smaller than the corresponding factor for the linearized problem (2.7) with x_1 independent perturbations. We conclude that x_2-independent perturbations seem to be less significant than x_1-independent perturbations, and thus conclude that the Orr-Sommerfeld equations do not seem to be so relevant in initial transition to turbulence in shear flow.

3. Transition to turbulence in shear flow

In this section we present aspects of transition to turbulence in parallel flow including a simple model for transition in pipe flow, and computational results for pipe flow and Couette flow. As a general reference into the large literature on transition, we refer to [3]. Our own early speculations are presented in [1] and [2].

3.1. An ode-model for transition.

We consider the following initial value problem for a system of two ordinary differential equations: find $w(t) = (w_1(t), w_2(t))$ such that

$$\begin{aligned} \dot{w}_1 + \nu w_1 - \lambda w_1 w_2 &= \nu \qquad t > 0, \\ \dot{w}_2 + 2\nu w_2 - \nu w_2 w_1 &= 0 \qquad t > 0, \\ w_1(0) = 1, \quad w_2(0) &= \kappa\nu, \end{aligned} \tag{3.1}$$

where ν is a small positive parameter, and λ and κ are positive parameters of moderate size. The system (3.1) models almost parallel shear flow with w_1 representing the flow velocity in the main direction of the flow, and w_2 the small velocities transversal to the main flow, and the stationary solution $w = (1, 0)$ corresponds to Couette flow between two plates or Poiseuille flow in a pipe. We shall use the model to describe how the small perturbation $\kappa\nu$ of w_2 may cause the base solution $(1, 0)$ to become unstable if $\lambda\kappa$ is larger than some critical value of moderate size.

We shall see that the model (3.1) contains an essential part of the secret of transition to turbulence in parallel flow. The equations for w_1 and w_2 in (3.1) are coupled through the quadratic terms $\lambda w_1 w_2$ and $\nu w_1 w_2$, and model the following selection of terms from the Navier-Stokes equations

$$\begin{aligned} \dot{u}_1 - \nu\Delta u_1 + u_{1,2}u_2 &= \nu \qquad t > 0, \\ \dot{u}_2 - \nu\Delta u_2 + u_{2,1}u_1 &= 0 \qquad t > 0, \end{aligned} \tag{3.2}$$

from the momentum equations for the main flow velocity u_1 and the transversal velocity u_2. The nonlinear coupling terms $u_{1,2}u_2$ and $u_{2,1}u_1$ are modeled in the form $\lambda w_1 w_2$ and $\nu w_2 w_1$, corresponding to assuming that $u_{1,2} = -\lambda u_1$ and $u_{2,1} = -\nu u_2$, connecting transversal derivatives of u_1 with u_1 through the parameter λ, and the streamwise derivative of the transversal velocity $u_{2,1}$ with u_2 through the small parameter ν. The relation $u_{2,1} = -\nu u_2$ models a basic feature of parallel flow with the streamwise variations being small. Since we assume initially that $u_2 \approx w_2 \approx \nu$, it corresponds to assuming $u_{2,1} \sim \nu^2$, which is indeed very small. On the other hand, the assumption that $u_{1,2} = -\lambda u_1$ with λ of moderate size corresponds to a natural transversal variation of moderate size of the streamwise velocity in a shear flow.

Note that the coupling term $u_{1,1}u_1$ in the equation for u_1 is not modeled in the form of some multiple of w_1^2. This is because (a) assuming $u_{1,1} \approx \nu^2$, with a corresponding very small term $-\nu^2 w_1^2$ in the model, has no destabilizing effect, and (b) assuming $u_{1,1} = -C\nu$ with a corresponding larger term $-C\nu w_1^2$, which may cause exponential growth through self-resonance in w_1, is not realistic. In fact, (b) is more or less the classical scenario based on the 2d Orr-Sommerfeld equations, which require artificially generated perturbation levels in experiments, for example through heavily vibrating ribbons.

In the transition model, we thus seek to build in realistic features of shear flow including realistic perturbation levels. If we assume zero perturbations, then the model reduces to $\dot{w}_1 + \nu w_1 = 0$, $\dot{w}_2 + 2\nu w_1 = 0$, which has no chance of going unstable. If we assume large perturbation levels, then instability may result immediately. However, none of these scenarios occur in reality, and the role of the model is to explain how small but realistic size perturbations, indeed may cause the initially stable base flow to go unstable after some time. Our model builds on the presence of a very small perturbation of order ν^2 of the transversal velocity in the streamwise direction, which naturally may be introduced through the roughness of the pipe. The model does not build on a larger variation of order ν of the streamwise velocity in the streamwise direction, which only seems to be possible with artificially generated perturbations.

The model (3.1) contains the two basic parameters λ and κ, both of moderate size, λ being related to the transversal geometry of the flow such as pipe cross section, $\kappa\nu$ representing a perturbation level in transversal velocities, and $\kappa\nu^2$ a perturbation level in streamwise derivatives of transversal velocities, including both transversal and streamwise perturbations levels. We will see that if $\lambda\kappa$ is larger than some critical value of moderate size, then transition to instability will take place in the model. This indicates that transition in shear flow builds on a combination of features related the transversal geometry and levels of perturbations in both transversal and streamwise direction. We give below computational results for transition in pipe flow supporting this picture.

The system (3.1) has two stationary solutions $w = (1, 0)$ and $w = (2, \nu/(2\lambda))$, with $(1, 0)$ representing the basic Couette or Poiseuille flow. A classical stability analysis based on the eigenvalues of the corresponding linearized system, indicates that $(1, 0)$ is stable and $(2, \nu/(2\lambda))$ is unstable. For example, the linear system obtained linearizing around $(1, 0)$, takes the form

$$
\begin{aligned}
\dot\varphi_1+\nu\varphi_1-\lambda_1\varphi_2 &= \nu \qquad t>0,\\
\dot\varphi_2+\nu\varphi_2 &= 0 \qquad t>0,\\
\varphi_1(0)=\varphi_{10},\quad \varphi_2(0) &= \varphi_{20},
\end{aligned}
\tag{3.3}
$$

where the coefficient matrix $A=[\nu\ \ -1, 0\ \nu]$ has a double positive eigenvalue ν. The corresponding coefficient matrix linearizing around $(2,\nu/(2\lambda))$, has one positive (stable) and one negative (unstable) eigenvalue. A classical stability analysis shows that $(1,0)$ is stable under sufficiently small perturbations, and that $(2,\nu/(2\lambda))$ is unstable even under small perturbations. As a result $(1,0)$ is unstable under large perturbations bringing the initial value sufficiently close to the unstable solution $(2,\nu/(2\lambda))$. However, the classical eigenvalue stability analysis is unable to explain the intriguing fact that $(1,0)$ may become unstable even under a small perturbation of the initial data $(1,0)$, if we just have patience to wait! We will now present such a scenario of transition, where the stationary solution $(1,0)$ of (3.1) goes unstable under a small perturbation of initial data of the form $(0,\kappa\nu)$, where κ is a parameter of moderate size, and the scaling with ν makes the perturbation small (since we assume ν to be small). We shall see that if the product $\lambda\kappa$ is above a certain threshold of moderate size, then transition to instability will take place, if we wait over a period of time of length ν^{-1}.

We thus consider the problem (3.1) with the initial data $(1,\kappa\nu)$ close to $(1,0)$, and we ask if the corresponding solution $\bar w(t)$ may become unstable after some time. We see that $\dot{\bar w}_1(0)/\bar w_1(0)=\lambda\kappa\nu$, while $\dot{\bar w}_2(0)/\bar w_2(0)=-\nu$, which shows that initially $\bar w_1$ grows and $\bar w_2$ decays at rates $\propto\nu$. Now, $\bar w_1$ will continue to grow at that rate as long as $\lambda\bar w_2>\nu$, and further $\bar w_2$ will start to grow as soon as $\bar w_1>2$. Thus, if $\bar w_1$ manages to become larger than 2, before $\bar w_2$ has decayed below ν/λ, then both components will propel each other to infinity, corresponding to instability. We shall see that this will occur if $\lambda\kappa$ is above a certain threshold. We notice that the time scale for significant changes in both $\bar w_1$ and $\bar w_2$ is $\sim\nu^{-1}$, which is a long time since ν is small. The scenario is thus that $\bar w_1$ grows slowly at the rate ν over a long time, and if $\lambda\kappa$ is above the threshold, then $\bar w_1$ may reach the value 2, where also $\bar w_2$ starts to grow after which a blow up follows on a usually somewhat shorter time scale (though still $\propto\nu^{-1}$). This scenario is easy to grasp intuitively, and conforms with the every-day experience of quit sudden blow-up, as a result of an accumulation of small events over a long period.

Solving the linearized equation (3.3) approximately describing the evolution of $\bar w-(1,0)$, we find that

$$
\bar w_1(t)\approx 1+\varphi_1=1+\lambda\kappa t\nu\exp -t\nu,\quad \bar w_2(t)\approx\varphi_2=\kappa\nu\exp -t\nu,
\tag{3.4}
$$

which shows the slow growth of $\bar w_1$ and slow decay of $\bar w_2$ over the long time scale prior to the blow up, occuring if $\lambda\kappa$ is above the threshold. The linear growth in time of φ_1 may be viewed as a consequence of the non-normality of the coefficient matrix A. A classical stability analysis focussing on the double positive eigenvalue ν of $A=[\nu\ \ -1, 0\ \nu]$, states that the factor $t\exp -\nu t$ eventually will decay to zero as $t\to\infty$, but misses the substantial transient growth to the level $\propto\nu^{-1}$ after time $\propto\nu^{-1}$ prior to decay. This perturbation growth of size $\propto \nu^{-1}$ is capable of bringing a solution from the point $(1, \kappa\nu)$ very close to $(1, 0)$, into a neigborhood of the unstable point $(2, \nu(2\lambda))$ with ensuing blow up.

3.2. **Computational transition in Couette and Poiseuille flow.** To verify that the predictions of the model (3.1) applies in the case of shear flow we present computational results for two test problems: transition to turbulence in Couette and Poiseuille flow in a pipe along the x_1-axis with square cross section 1×1, assuming periodicity in the streamwise direction. We use the cG(1)cG(1)-method (linear, continuous finite element approximation in space and time)on a regular tetrahedral mesh with meshsize $h = 1/64$. For both cases we start with a small initial transversal velocity perturbation $\varphi^0 = (0, \varphi_2^0(x_2, x_3), \varphi_3^0(x_2, x_3))$, with $\varphi_2^0(x_2, x_3) = \nu \sin(2\pi x_2)\cos(\pi x_3)$ and $\varphi_2^0(x_2, x_3) = -\nu\cos(2\pi x_2)\sin(\pi x_3)$, where $\nu = 0.1$. We also apply a very small x_1-dependent driving force $f = (0, f_2(x_1), f_3(x_1))$, with $f_2(x_1) = f_3(x_1) = 10^{-3}\sin(10\pi x_1)$, creating and sustaining a very small streamwise variation, modeling, for example, imperfections in the pipe.

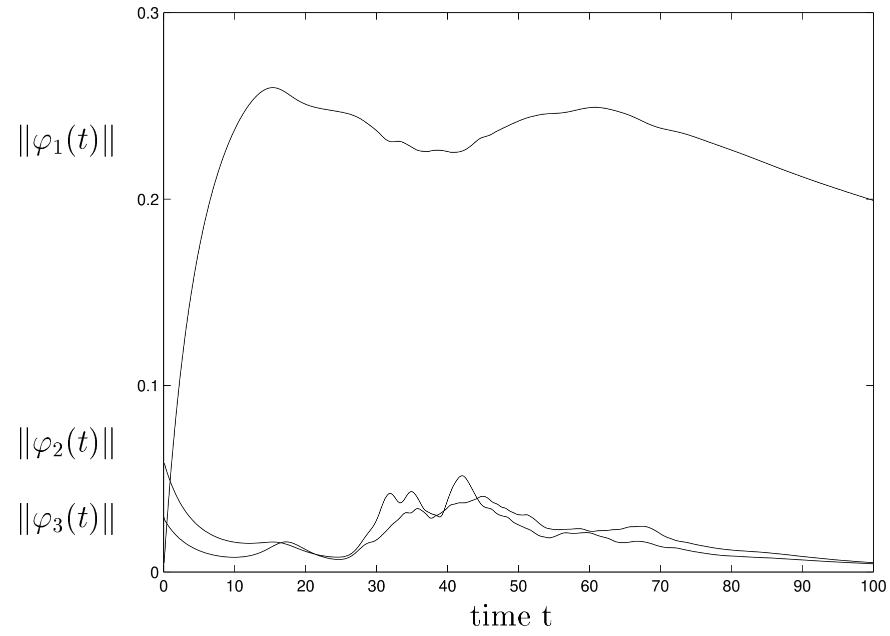

FIGURE 1. Couette flow: Pertubations

The Couette base flow $u = (u_1, 0, 0)$ has a streamwise velocity profile $u_1 = 2x_2 - 1$, with streamwise velocity ± 1 on the top and bottom, slip side walls, and periodic boundary conditions in the streamwise direction. Initially, as in the scenario predicted by the model (3.1), the streamwise pertubation φ_1 grows linearly through the action of the Taylor-Görtler mechanism, see Fig.1. In Fig.2 we can see the formation of high velocity streaks due to the Taylor-Görtler mechanism, shifting particles with different streamwise velocities causing the formation of high and low velocity streaks. The pertubations φ_2 and φ_3 decreases

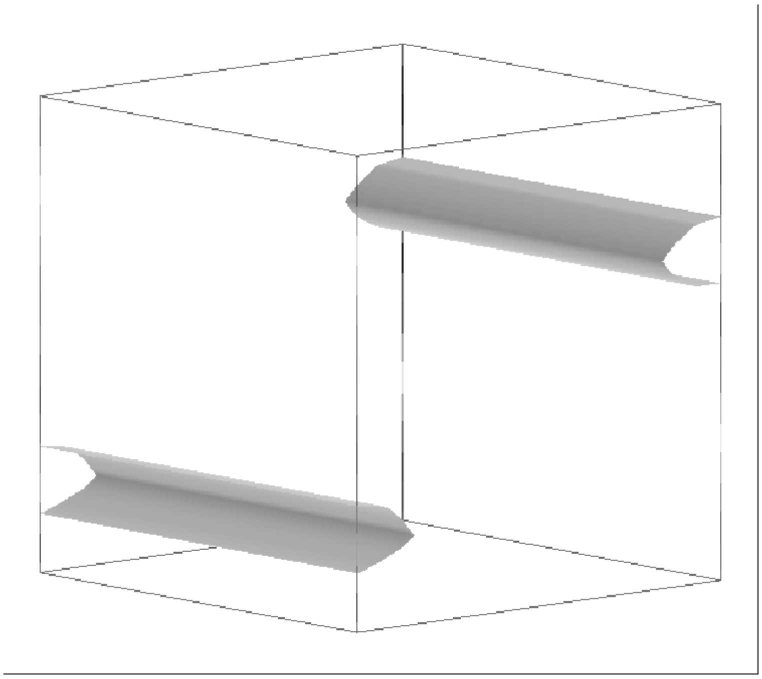

FIGURE 2. Couette flow: Isoconcentration surfaces for φ_1 prior to the transistion, corresponding to high speed streaks

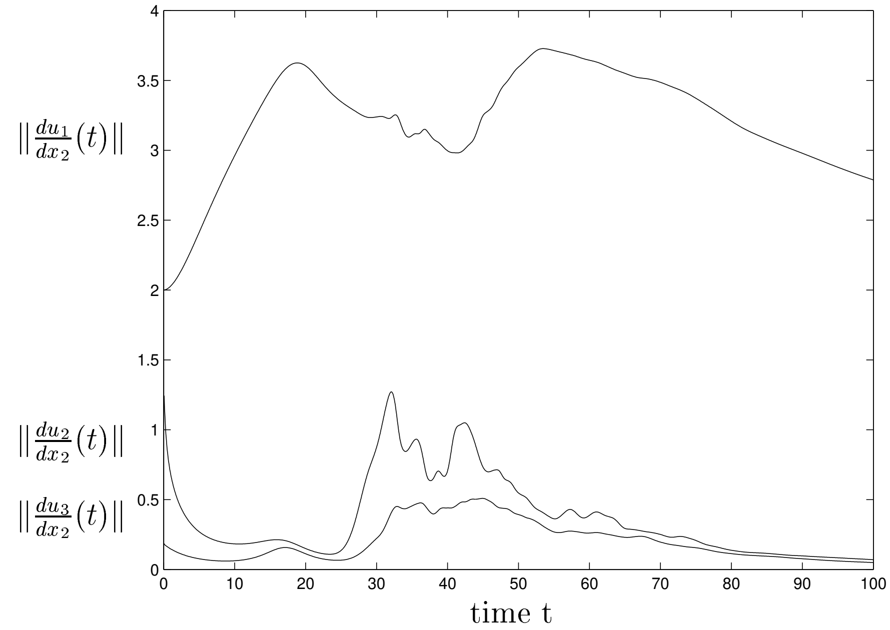

FIGURE 3. Couette flow: x_2-derivatives

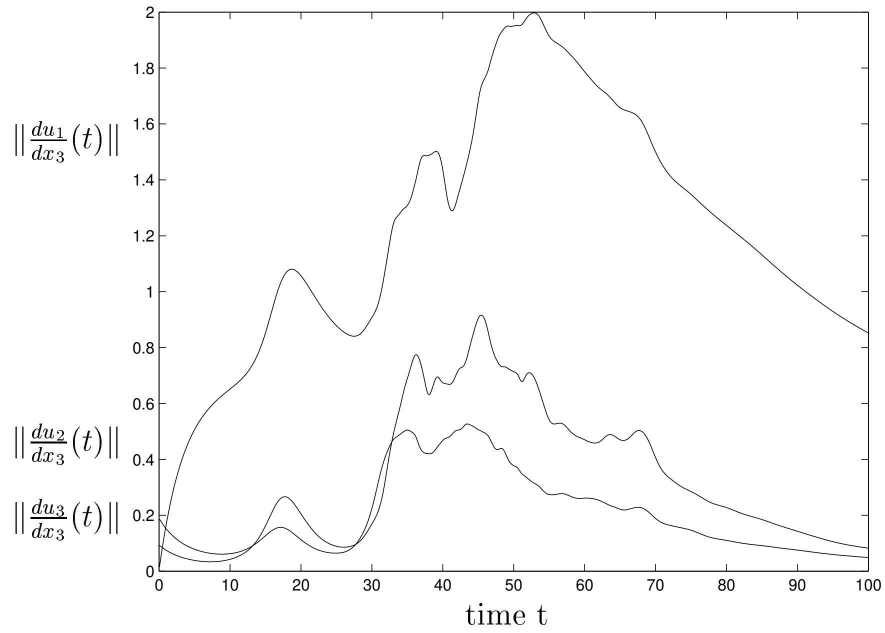

FIGURE 4. Couette flow: x_3-derivatives

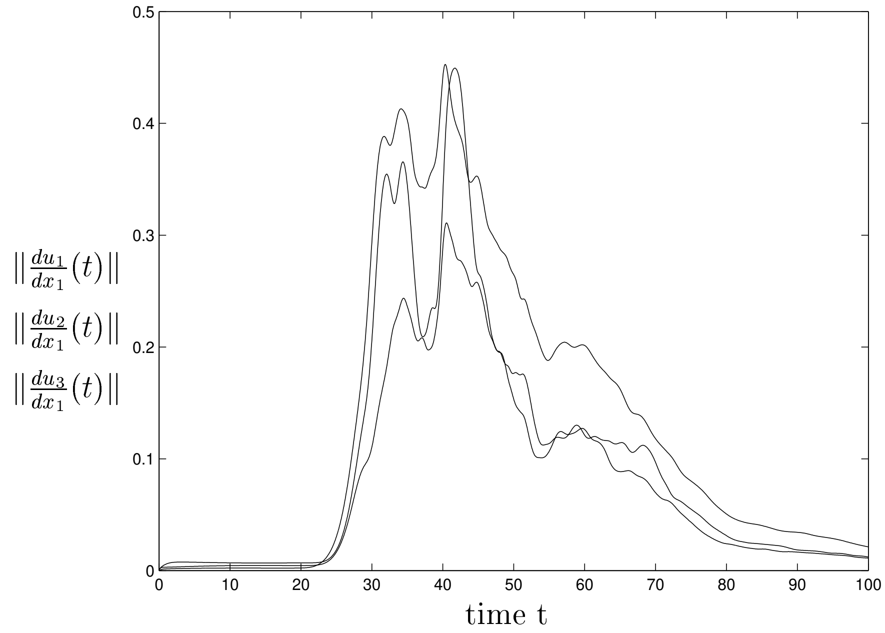

FIGURE 5. Couette flow: x_1-derivatives

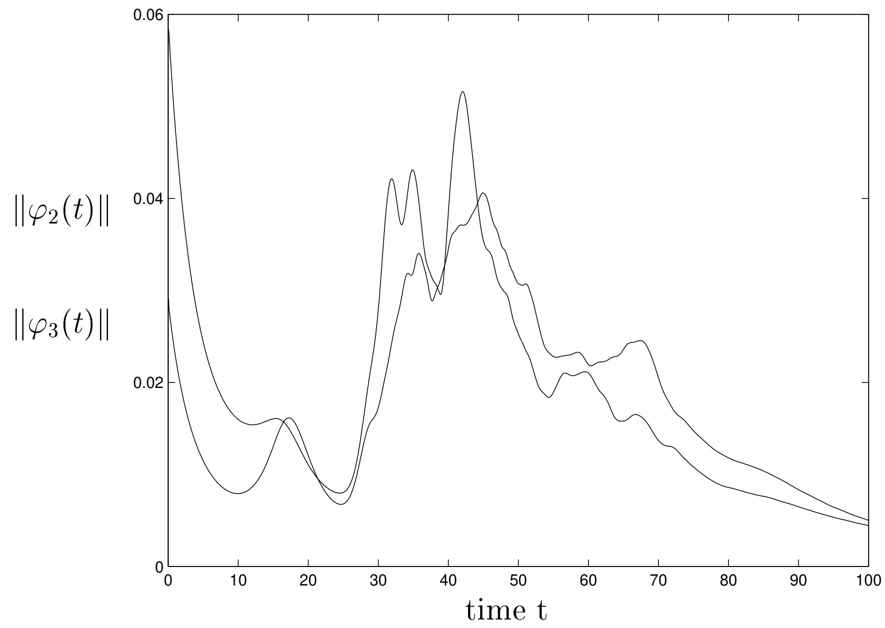

FIGURE 6. Couette flow: x_2- and x_3-pertubations

initially as predicted by the model (3.1). In the same way, derivatives with respect to x_2 and x_3 grow linearly for u_1, and decreases for u_2 and u_3 (see Figs.3-4). In Fig.5 we see that near $t = 25$ we get a sudden burst where all x_1-derivatives increase by a factor 100 over a short time interval, corresponding to initial transition. We also get a sudden increase in φ_2 and φ_3, see Fig.6, at the same time. A key observation is that the transition is not possible until the pertubation φ_1 and the derivatives $\partial u_1/\partial x_2$ and $\partial u_1/\partial x_3$ has reached a certain threshold. Another important observation which is not obvious from studying the global norms is that the pertubations of course vary in space, and that the threshold is a local condition that has to be satisfied. In Fig.7 we can follow the initial phase of the transition.

The Poiseuille base flow has a streamwise velocity profile $u_1(x_2, x_3) = 16y(1-y)z(1-z)$ in a channel with no slip walls and a force term $f = (32(y(1-y)+z(1-z)), 0, 0)$, where we use periodic boundary conditions in the streamwise direction. In Fig.8 we show the perturbation growth in the L_2-norm and note a linear growth in the streamwise pertubation corresponding to the Taylor-Görtler mechanism, whose action is shown in Fig.10 slowly shifting particles with different streamwise velocity transversally with a considerable reorganization of the streamwise velocity from the transversal perturbation. Fig.9 shows the L_2-norm of the x_1-derivatives in the solution as a function of time, with a sudden increase near $t = 6$. Again we note that this increase is not possible until the x_1-pertubation φ_1 is large enough.

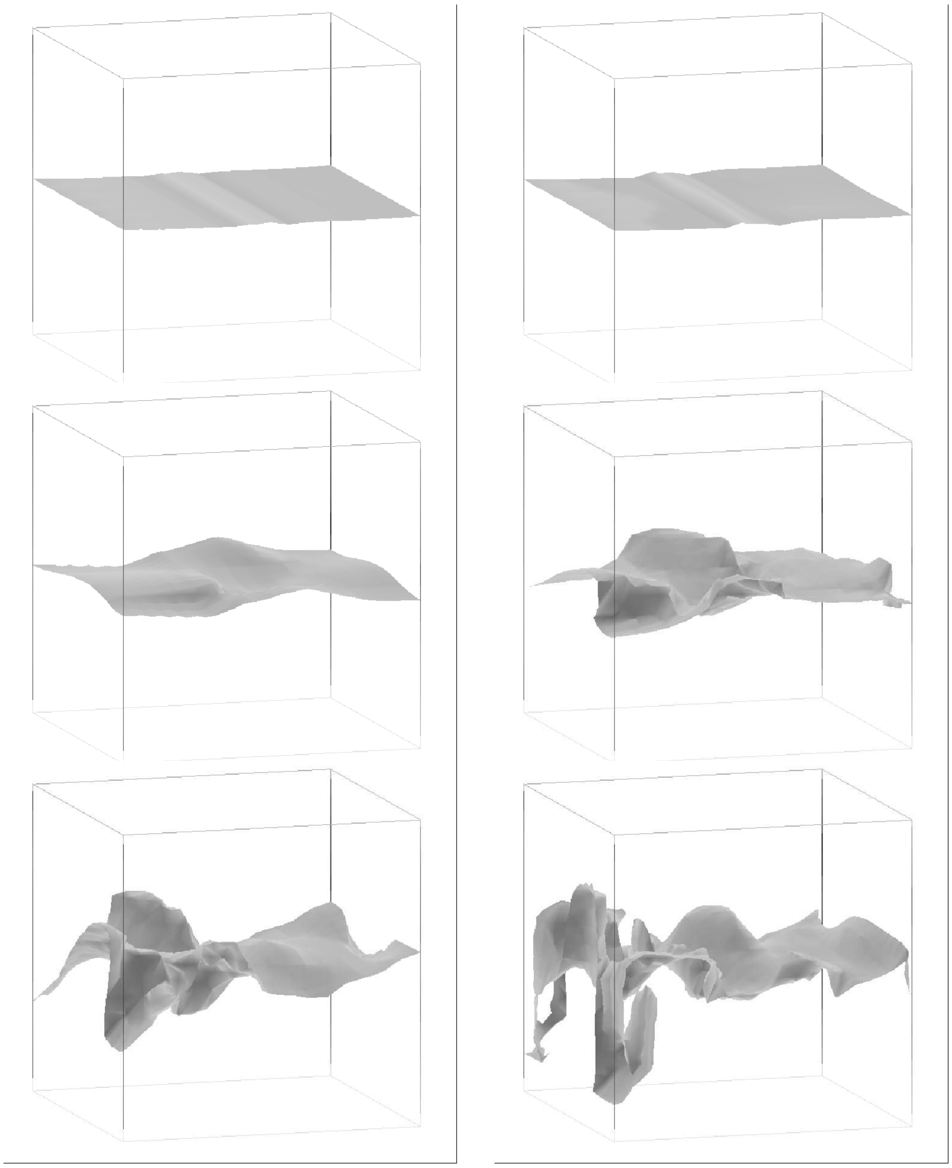

FIGURE 7. Streamwise velocity zero isosurfaces in Couette flow for $t = 20, 25, 30, 32, 34, 40$, showing the initial phase of the transition

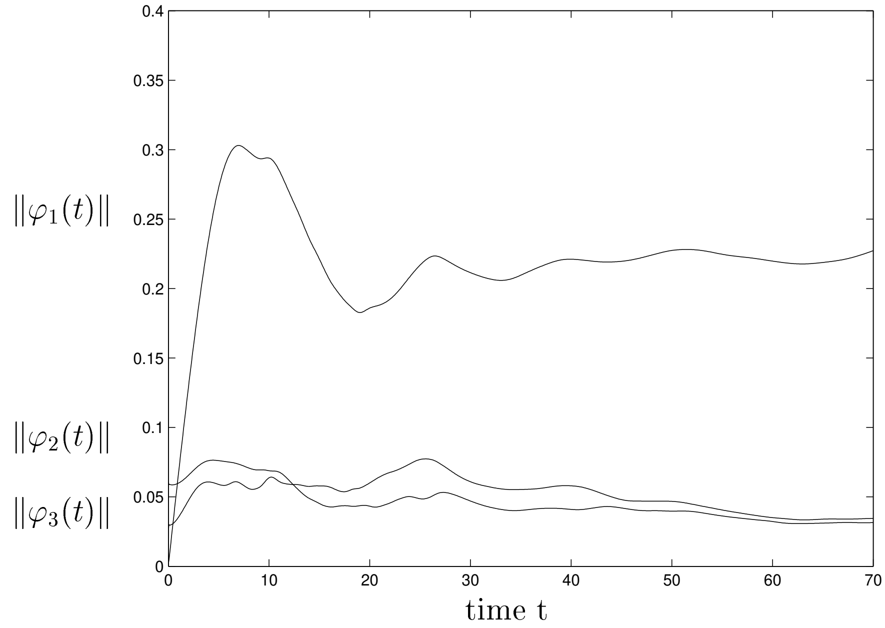

FIGURE 8. Poiseuille flow: Pertubations

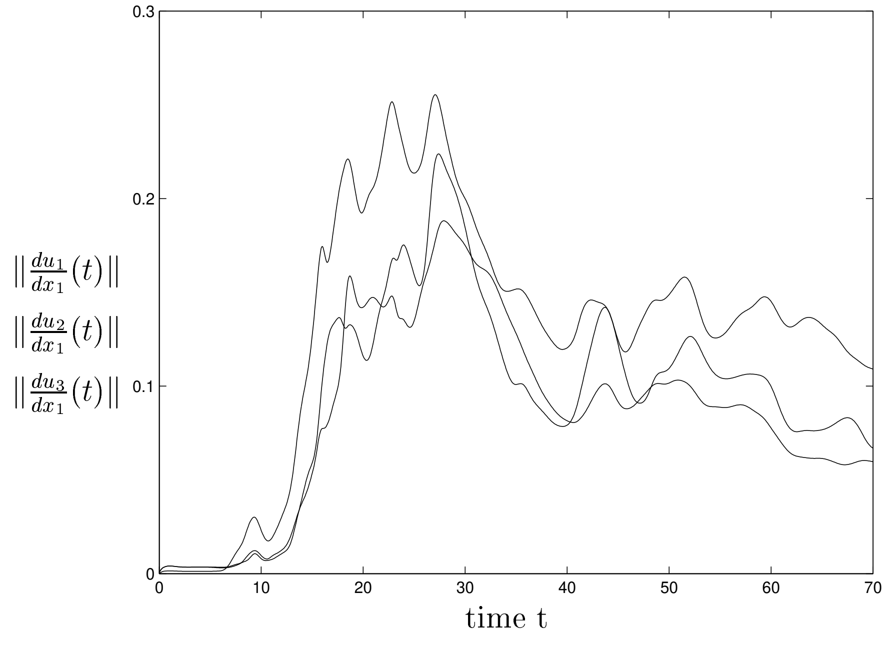

FIGURE 9. Poiseuille flow: x_1-derivatives

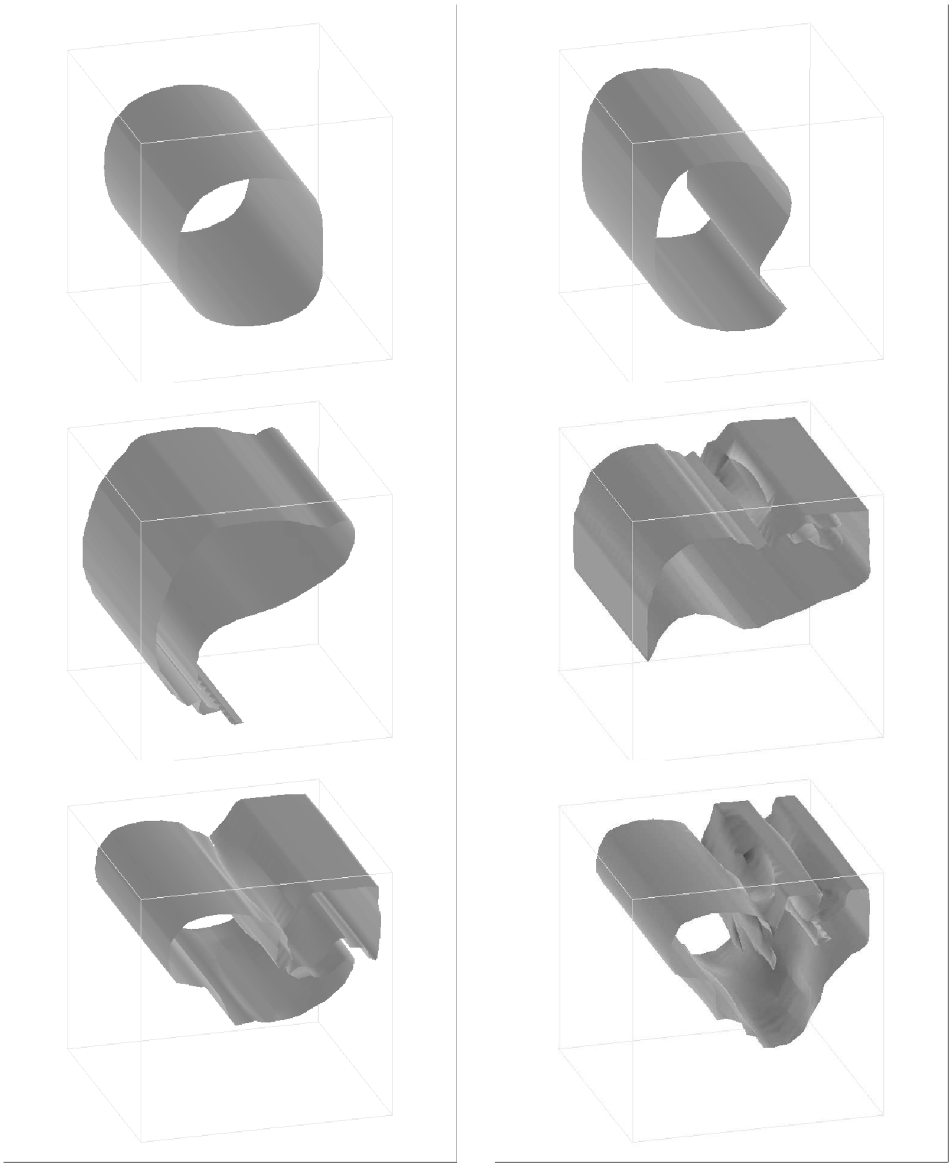

FIGURE 10. Streamwise velocity isosurfaces in Poiseuille flow at $t = 1, 3, ..., 15$, illustrating the Taylor-Görtler mechanism

We note that while the computations are valid in the initial phase of the transition, the computational mesh is too coarse for an accurate *direct numerical simulation* (DNS) of the turbulent flow following the transition. To be able to compute turbulent flows we either need a very fine mesh, resolving the finest scales in the flow, or a turbulence model of some sort.

References

[1] C. Johnson, R. Rannacher and M. Boman (1995) On transition to turbulence and error control in CFD, Preprint 95-06, SFB 359, Univ. of Heidelberg.

[2] C. Johnson and R. Rannacher. (1995) Numerics and hydrodynamic stability: Towards error control in CFD, SIAM J. Numer. Anal., 32, pp 1058-1079.

[3] P. Schmid and D. Henningson. (2001) *Stability and Transition in Shear Flows*, Applied Mathematical Sciences 142, Springer.

Chalmers Finite Element Center Preprints

2000–01 *Adaptive finite element methods for the unsteady Maxwell's equations*
Johan Hoffman

2000–02 *A multi-adaptive ODE-solver*
Anders Logg

2000–03 *Multi-adaptive error control for ODEs*
Anders Logg

2000–04 *Dynamic computational subgrid modeling (Licentiate Thesis)*
Johan Hoffman

2000–05 *Least-squares finite element methods for electromagnetic applications (Licentiate Thesis)*
Rickard Bergström

2000–06 *Discontinuous galerkin methods for incompressible and nearly incompressible elasticity by Nitsche's method*
Peter Hansbo and Mats G. Larson

2000–07 *A discountinuous Galerkin method for the plate equation*
Peter Hansbo and Mats G. Larson

2000–08 *Conservation properties for the continuous and discontinuous Galerkin methods*
Mats G. Larson and A. Jonas Niklasson

2000–09 *Discontinuous Galerkin and the Crouzeix-Raviart element: application to elasticity*
Peter Hansbo and Mats G. Larson

2000–10 *Pointwise a posteriori error analysis for an adaptive penalty finite element method for the obstacle problem*
Donald A. French, Stig Larson and Ricardo H. Nochetto

2000–11 *Global and localised a posteriori error analysis in the maximum norm for finite element approximations of a convection-diffusion Problem*
Mats Boman

2000–12 *A posteriori error analysis in the maximum norm for a penalty finite element method for the time-dependent obstacle problem*
Mats Boman

2000–13 *A posteriori error analysis in the maximum norm for finite element approximations of a time-dependent convection-diffusion problem*
Mats Boman

2001–01 *A simple nonconforming bilinear element for the elasticity problem*
Peter Hansbo and Mats G. Larson

2001–02 *The $\mathcal{LL}^*$ finite element method and multigrid for the magnetostatic problem*
Rickard Bergström, Mats G. Larson, and Klas Samuelsson

2001–03 *The Fokker-Planck operator as an asymptotic limit in anisotropic media*
Mohammad Asadzadeh

2001–04 *A posteriori error estimation of functionals in elliptic problems: experiments*
Mats G. Larson and A. Jonas Niklasson

2001–05 *A note on energy conservation for Hamiltonian systems using continuous time finite elements*
Peter Hansbo

2001–06 *Stationary level set method for modelling sharp interfaces in groundwater flow*
Nahidh Sharif and Nils-Erik Wiberg

2001–07 *Integration methods for the calculation of the magnetostatic field due to coils*
Marzia Fontana

2001–08 *Adaptive finite element computation of 3D magnetostatic problems in potential formulation*
Marzia Fontana

2001–09 *Multi-adaptive galerkin methods for ODEs I: theory & algorithms*
Anders Logg

2001–10 *Multi-adaptive galerkin methods for ODEs II: applications*
Anders Logg

2001–11 *Energy norm a posteriori error estimation for discontinuous Galerkin methods*
Roland Becker, Peter Hansbo, and Mats G. Larson

2001–12 *Analysis of a family of discontinuous Galerkin methods for elliptic problems: the one dimensional case*
Mats G. Larson and A. Jonas Niklasson

2001–13 *Analysis of a nonsymmetric discontinuous Galerkin method for elliptic problems: stability and energy error estimates*
Mats G. Larson and A. Jonas Niklasson

2001–14 *A hybrid method for the wave equation*
Larisa Beilina, Klas Samuelsson and Krister Åhlander

2001–15 *A finite element method for domain decomposition with non-matching grids*
Roland Becker, Peter Hansbo and Rolf Stenberg

2001–16 *Application of stable FEM-FDTD hybrid to scattering problems*
Thomas Rylander and Anders Bondeson

2001–17 *Eddy current computations using adaptive grids and edge elements*
Y. Q. Liu, A. Bondeson, R. Bergström, C. Johnson, M. G. Larson, and K. Samuelsson

2001–18 *Adaptive finite element methods for incompressible fluid flow*
Johan Hoffman and Claes Johnson

2001–19 *Dynamic subgrid modeling for time dependent convection–diffusion–reaction equations with fractal solutions*
Johan Hoffman

2001–20 *Topics in adaptive computational methods for differential equations*
Claes Johnson, Johan Hoffman and Anders Logg

2001–21 *An unfitted finite element method for elliptic interface problems*
Anita Hansbo and Peter Hansbo

2001–22 *A P^2–continuous, P^1–discontinuous finite element method for the Mindlin-Reissner plate model*
Peter Hansbo and Mats G. Larson

2002–01 *Approximation of time derivatives for parabolic equations in Banach space: constant time steps*
Yubin Yan

2002–02 *Approximation of time derivatives for parabolic equations in Banach space: variable time steps*
Yubin Yan

2002–03 *Stability of explicit-implicit hybrid time-stepping schemes for Maxwell's equations*
Thomas Rylander and Anders Bondeson

2002–04 *A computational study of transition to turbulence in shear flow*
Johan Hoffman and Claes Johnson

These preprints can be obtained from

`www.phi.chalmers.se/preprints`